Hindawi
International Journal of Aerospace Engineering
Volume 2019, Article ID 2030617, 12 pages
https://doi.org/10.1155/2019/2030617

Research Article

Guaranteeing Prescribed Performance Control for Gyrostabilized Platform with Unknown Control Direction Preceded by Hysteresis

Yexing Wang,[1] **Humin Lei**,[1] **Jikun Ye**,[1] **Xiangwei Bu**,[1] **and Yali Xue**[2]

[1]*Air and Missile Defense College, Air Force Engineering University, Xi'an 710051, China*
[2]*College of Automation, Nanjing University of Aeronautics and Astronautics, Nanjing 211100, China*

Correspondence should be addressed to Yexing Wang; 1216352604@qq.com and Jikun Ye; jikunbo@sina.com

Received 17 July 2018; Revised 1 September 2018; Accepted 10 October 2018; Published 16 January 2019

Academic Editor: Kenneth M. Sobel

This paper investigates the problem of precise and quick tracking for gyrostabilized platform (GSP) with unknown hysteresis, unknown control directions, and unknown compound disturbance. Firstly, the dynamic model of GSP is transformed into a strict feedback formulation by designed FD to facilitate the backstepping control system. Secondly, performance functions are constructed at each step of backstepping design to force tracking errors to fall within the prescribed boundaries. Besides, through ingenious transformation, radial basis function neural network (RBFNN) is applied to estimate the unknown control gains preceded by hysteresis. Hence, the problem of prescribed performance control with unknown compound disturbances, unknown hysteresis, and unknown control directions is creatively solved. Furthermore, the exploited controllers are accurate model independent, which guarantees satisfactory robustness of control laws against unknown uncertainties. Finally, the stability of the closed-loop control system is confirmed via Lyapunov stability theory, and numerical simulations are given for a GSP to validate the effectiveness of the proposed controller.

1. Introduction

Gyrostabilized platform (GSP) is a kind of precise servo tracking system, which is usually mounted on a mobile carrier for stable tracking of moving targets. Varieties of detectors are mounted on GSP to isolate the motion of carrier as well as to get high-performance information of targets. GSP is originally used in weapons including nonstrapdown seekers [1], aerial shooting, and airborne remote sensing system [2]. Recently, it is also widely used in robotics [3], deep space exploration, and other high-precision tracking systems. Therefore, it has broad application prospects, and it is worth to investigate further.

GSP is a complex time-varying nonlinear system with compound disturbances [4, 5]. The internal disturbances of system include hysteresis nonlinearity of motor and the perturbation of model, while the external disturbances of system include the motion of basement and friction torque between the shafts. Faced with such problems, researches have tried varieties of approaches to realize better dynamic response performance and stronger robustness of GSP. For most actual GSP system, proportional-integral-derivative (PID) control or modified PID has been widely used because of its reliability and simple control structure [6].

Recently, to solve the problem of compound disturbances, many control strategies have been designed [7]. Active disturbance rejection control technique is commonly used to compensate for disturbance because of its strong robustness against various disturbances, X. Y. Zhou and et al. combine the feedforward control with friction observer to compensate for friction disturbance, and the friction is eliminated in large scale because of the precise estimation. Besides, they designed a backstepping integral adaptive compensator to compensate for disturbance [8, 9]. While the shortcoming is that the parameters of friction are estimated offline. Moreover, RBFNN is commonly used to estimate the disturbance for its approximation ability [10, 11]. In reference [11], an adaptive RBFNN was proposed to generate the feedback control parameters online, while the extended state observer is used to compensate

for composite disturbances. The control strategy eliminates disturbances in large scale, while the overshoot of response is large. In reference [12], an adaptive neural network is applied to estimate the uncertain disturbances as well as eliminating "chattering phenomenon," the strategy is simple and efficient.

Though satisfying robustness and high precision can be achieved through the abovementioned methods, there are still some shortcomings to these methods. A fatal one is that most researchers focus on the characteristic of controlled object, while the nonlinearity of actuator is ignored. The servo motor plays a role of actuator, its precision is mainly restrained by trigger deadzone and hysteresis, while the deadzone can be seen as external disturbance to eliminate. Many researchers have drawn a common conclusion that that hysteresis of motor will deteriorate its response characteristic and tracking precision [13, 14]. Therefore, to promote the performance of GSP, hysteresis problem has to be solved. Besides, the existing research focuses on improving steady performance of GSP. The robustness and precision of GSP are enhanced, but the dynamic performance of GSP cannot be guaranteed.

The study of hysteresis nonlinearities has been drawing much attention in the control community for a long time [15, 16]. For several classes of deterministic nonlinear system with unknown backlash-like hysteresis, adaptive control was proposed by some researchers, while the method has received little attention [17]. Nevertheless, few researchers investigate the problem with both unknown backlash-like hysteresis and unknown control directions [18]. In reference [18], Yu et al. adopt backstepping control to control the mentioned system. By designing a state observer, the states of transformed system are estimated, besides, a RBFNN is adopted to acquire estimated unknown functions, while the control strategy brings in two additional states, which makes controller design complex.

Motivated by previous investigations, this paper will concentrate on solving the problem of compound disturbances and unknown control directions as well as guaranteeing prescribed performance for tracking errors. The compound disturbances include two parts. One part is friction torque, which is a strong nonlinear disturbance that affects the tracking performance at angular velocity "crossing zero" point sharply [2]. And the other is the movement of basement. The disturbances are all considered unknown and estimated online by RBFNN. RBFNN plays a crucial part in disturbance compensation and enhancing the robustness. The key point of application of RBFNN is the model transformation. It is model transformation that normalizes the disturbances. Meanwhile, the designed FD enables transformation by estimating newly defined states. Furthermore, because of the high dynamic performance of GSP, prescribed performance control is adopted. Performance functions are defined under the structure of backstepping control. At the last step of backstepping control, there exists unknown control gain; therefore, a Nussbaum gain function (NGF) is adopted to solve the problem. Thus, prescribed performance control under compound disturbances and unknown control directions is creatively achieved.

Special contributions of this paper are summarized as follows:

(1) This paper focuses on the problem of compound disturbances for GSP. Different from existing researches on GSP, in this paper, hysteresis problem is creatively taken into account. Different from most investigations into hysteresis, the hysteresis is completely unknown. Especially, compared with reference [18], input-driven observer is not needed

(2) Prescribed output quality is guaranteed for GSP through prescribed performance control; the control strategy is creatively proposed and applied to GSP

(3) The presented control approach is independent of accurate models. Thus, its disturbance rejection ability is fine and the computational cost is relatively low

The paper is organised as follows: in Section 2, the model of GSP is built and its working preliminaries are presented. In Section 3, necessary control techniques are introduced, and the controller is designed along with the stability analysis. In Section 4, simulations are carried out to demonstrate the effectiveness.

2. System Modeling and Problem Formulation

2.1. Constitution and Operating Principle of Two-Axis GSP. Figure 1 shows the schematic diagram of two-axis GSP. We can see that stabilized platform consists of two gimbals, which are pitch gimbal and yaw gimbal, respectively. The system is driven by two servo motors; the detective sensor is placed in the inner frame.

From Figure 1, we can see the relationships between two gimbals: gyroscopes measuring the angular rate of pitch and yaw gimbals, angle sensors measuring the angle of pitch and yaw gimbals, and current sensors measuring the current of pitch and yaw motors.

GSP is fixed at the projectile body to track the target [19].

Because of the low coupling and similar characteristic of pitch and yaw channels [20], we choose pitch channel to analyze.

2.2. Dynamic Model of the GSP. Figure 2 shows the pitch channel block diagram of GSP. The block within the red imaginary line stands for the servo motor, while the block within the blue imaginary line stands for the friction disturbance; θ_d represents the angle conference signal of the system; k_{PWM} is the power amplifier coefficient; $\dot{\theta}$ is the angular rate of stabilized platform in inertial space; $\dot{\vartheta}$ is the disturbance of basement movement; T_{turb} is the disturbance moment; k_g is the simplified transfer function of rate gyroscope; T_c is the moment output of servo motor; i is the electric current of the servo motor; C_m is the moment coefficient of motor; C_e is the coefficient of counter electromotive force.

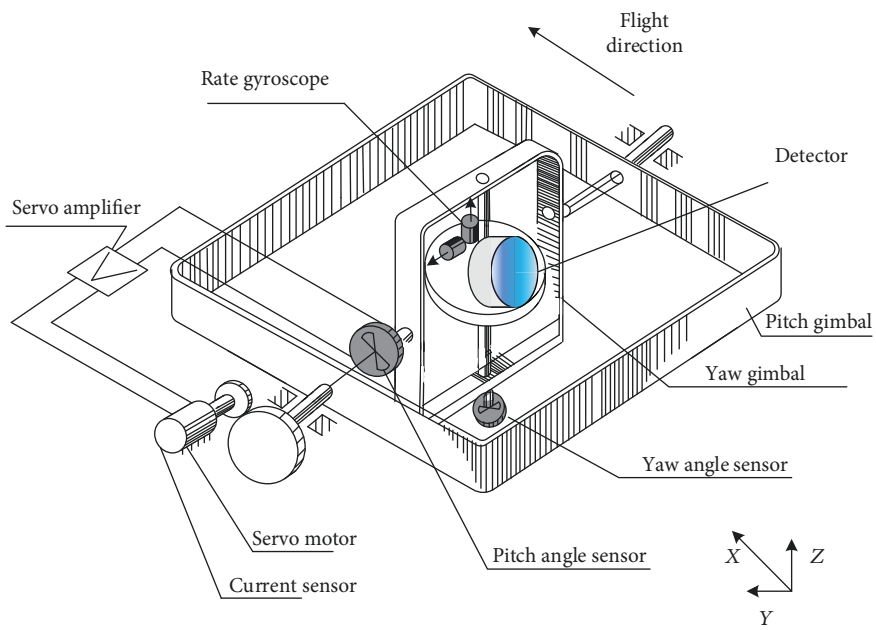

Figure 1: Schematic diagram of the two-axis GSP.

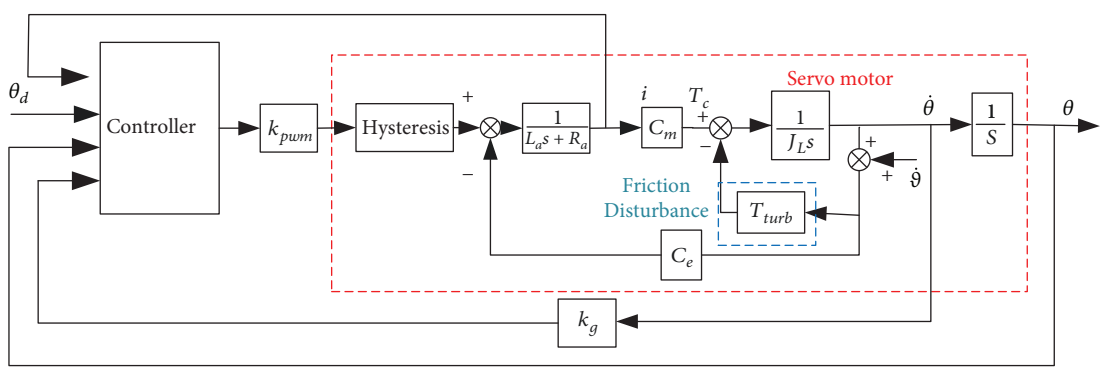

Figure 2: Block diagram of GSP tracking loop.

Combining with the dynamic equation of stable platform and the dynamic equation of motor, mathematical model of GSP is acquired as follows [21]:

$$\begin{cases} \dot{x}_1 = x_2, \\ \dot{x}_2 = \dfrac{C_m x_3}{J_L} - \dfrac{T_{\text{turb}}}{J_L}, \\ \dot{x}_3 = -\dfrac{C_e}{L_a} x_2 - \dfrac{R_a}{L_a} x_3 + \dfrac{k_{\text{PWM}}}{L_a} u(v) - \dfrac{C_e \dot{\vartheta}}{L_a}, \end{cases} \tag{1}$$

where x_1, x_2, and x_3 are state variables, which represent $\theta_l, \dot{\theta}_l$, and i, respectively. $u(v)$ is the system input and the output of the following backlash-like hysteresis described as [22]

$$\dot{u}(v) = \alpha |\dot{v}| (cv - u(v)) + B\dot{v}, \tag{2}$$

where v is the input of the backlash-like hysteresis, α and B are constants, and $c > 0$ is the slope of lines satisfying $c > B$. This paper assumes that the parameters of (2) are unknown.

In the light of the analysis in [18], (2) can be solved as

$$u(t) = cv(t) + d(v), \tag{3}$$

where

$$\begin{aligned} d(v) = {} & (u_0 - cv_0) e^{-\alpha(v - v_0)\ \text{sgn}\ (\dot{v})} \\ & + e^{-\alpha v\ \text{sgn}\ (\dot{v})} \int_{v_0}^{v} (B - c) e^{\alpha \varsigma\ \text{sgn}\ (\dot{v})} d\varsigma, \end{aligned} \tag{4}$$

where u_0 and v_0 are the initial values of u and v, respectively. As is shown in [21], $d(v)$ is bounded by an unknown constant value $d_{\max}$.

The disturbance torque mainly results from friction between gimbals [23]. Stribeck friction model is chosen as the torque disturbance model in this paper. The mathematical formulation is given as follows:

$$T_{\text{turb}} = \left[F_c + (F_s - F_c)e^{-(v/v_s)^2}\right] \operatorname{sgn}(v) + B_v v, \tag{5}$$

where F_c and F_s are Coulomb friction and static friction, respectively.

Remark 1. The controller output is v in Figure 2, while there exists unknown hysteresis, which can be expressed as $\dot{u}(v) = \alpha|\dot{v}|(cv - u(v)) + B\dot{v}$, is regarded as a completely unknown function. Thus, u in Figure 2 is regarded as the newly defined output of controller that drives the motor directly. The hysteresis makes the control directions unknown.

Remark 2. In this paper, "unknown hysteresis" means that in (3), the coefficient c and function $d(v)$ are unknown. "Unknown control directions" result from unknown hysteresis, as is shown in (1). In (1), the designed controller output is v, while the control item is $(k_{\text{PWM}}/L_a)u(v)$. The map from v to $u(v)$ is unknown, so the problem is called "problem with unknown control directions." "Unknown compound disturbances" mean that $T_{\text{turb}}, \dot{\vartheta}$ are completely unknown.

Remark 3. To enhance the control precision, some researchers identify the parameters of friction model [2, 24]. While the process of identification is complex owing to its complex dynamic behavior, besides, identification has to be carried out repeatedly for different systems. In this paper, friction torque is regarded unknown, which simplifies the process of controller design, and the algorithm is more universal to apply.

2.3. Control Problems for GSP. There are some troublesome characteristics in the GSP:

(1) When there exist unknown disturbances, high-performance angle tracking is hard to guarantee

(2) The unknown hysteresis results in unknown control direction problem for GSP, which increases the difficulty of controller design

3. Controller Design

3.1. Finite-Time-Convergent Tracking Differentiator Design. To estimate newly defined states, a finite-time tracking differentiator (FD) is designed.

Assumption 1 (see [25]). The input signal $x(t)$ is continuous and piecewise n-order derivable with the following characteristics. The derivatives of $x(t)$ up to order $n-2$ exist on the whole time domain and $x(t)$ is not $n-1$ order at some instants $t_j, j = 1, 2, \dots k$ may hold.

Based on the assumption, to estimate newly defined states, a high-order tracking differentiator (FD) is designed. The FD is formulated as follows:

$$\begin{aligned}
\dot{\chi}_1 &= \chi_2 \\
\dot{\chi}_2 &= \chi_3 \\
&\vdots \\
\dot{\chi}_i &= R^n\left[-a_1 \tanh(\chi_1 - x(t)) - a_2 \tanh\left(\frac{\chi_2}{R}\right)\right. \\
&\quad \left. - \cdots - a_i \tanh\left(\frac{\chi_i}{R^{n-1}}\right)\right].
\end{aligned} \tag{6}$$

Based on reference [26], there exist $\phi > 0$ and $\iota\phi > n$ such that $\chi_i - x^{(i-1)}(t) = O((1/R)^{\iota\phi - i + 1}), i = 1, 2, \dots, n$ where $R > 0$, $a_i > 0, i = 1, 2, \dots n$ are positive constants to be designed; $O((1/R)^{\iota\phi - i + 1})$ means the approximation of $(1/R)^{\iota\phi - i + 1}$ order between χ_i and $x^{(i-1)}(t)$; $\phi = (1 - \varpi)/\varpi$ and $x(t)$; $\varpi \in (0, \min\{\iota/(\iota + n)1/2), n \geq 2$ $x(t)$ is the input signal; $\chi_i, i = 1, 2, \dots, n$ donate the states of FD and they are $x^{(i-1)}(t), i = 1, 2, \dots, n$, respectively. The corresponding estimation errors are defined as follows:

$$s_1 = \chi_1 - x(t), s_2 = \chi_2 - \dot{x}(t), \dots, s_n = \chi_n - x^{(n-1)}(t). \tag{7}$$

The designed FD is proven finite-time-convergence and stable in reference [20], and the estimation error is bounded.

3.2. Neural Network. To guarantee the controller's robustness, an adaptive RBFNN is introduced to approximate the uncertain functions. The adaptive RBFNN is defined as the mapping relationship between input vector $\mathbf{X} = [x_1, x_2, \dots, x_n]^T \in \mathbf{R}^n$ and the output $y \in \mathbf{R}$ [26, 27].

$$y = \mathbf{W}^T \mathbf{h}(\mathbf{X}), \tag{8}$$

where $\mathbf{W} = [w_1, w_2, \dots, w_m]^T \in \mathbf{R}^m$ stands for weight vector; m and n represent the node number and input number, respectively; $\mathbf{h}(\mathbf{X}) = [h_1(\mathbf{X}), h_2(\mathbf{X}), \dots h_m(\mathbf{X})]^T \in \mathbf{R}^m$ with $h_j(\mathbf{X})$ is defined as follows:

$$h_j(\mathbf{X}) = \exp\left(-\frac{\|\mathbf{X} - c\|}{\sigma_j^2}\right) \in \mathbf{R}^m, \quad j = 1, 2, \dots, m, \tag{9}$$

where $c = [c_1, c_2, \dots, c_n]^T \in \mathbf{R}^m$ and $\boldsymbol{\sigma} = [\sigma_{j1}, \sigma_{j2}, \dots, \sigma_{jn}]^T \in \mathbf{R}^n$ mean a center and a width vector of $h_j(\mathbf{X})$, respectively [28, 29].

For an arbitrary continuous unknown function $F(\mathbf{X})$, it has to be proven that there exists an ideal weight vector $\mathbf{W} = [w_1, w_2, \dots, w_m]^T \in \mathbf{R}^m$ such that

$$F(\mathbf{X}) = \mathbf{W}^* \mathbf{h}(\mathbf{X}) + \varepsilon, \tag{10}$$

where ε is approximate error, which satisfies that $|\varepsilon| \le \varepsilon_{\max}$. It should be noted that $\mathbf{W}^*$ is unknown, its elements $w_1{}^*$, $w_2{}^*, \dots, w_m{}^*$ are required to be adjusted adaptively.

Define the error between the ideal weight vector W^* and the estimated weight vector $\widehat{\mathbf{W}}$ as

$$\tilde{\mathbf{W}} = \widehat{\mathbf{W}} - \mathbf{W}^*. \tag{11}$$

The adaptation laws of $\widehat{\mathbf{W}}$ is designed in next section.

3.3. Prescribed Performance. By prescribed performance, we mean that the tracking error e evolves strictly within the prescribed decaying bounds as follows:

$$-\underline{\delta}\hbar(t) < e(t) < \overline{\delta}\hbar(t), \tag{12}$$

where the performance function $\hbar(t) = (\hbar_0 - \hbar_\infty)e^{-lt} + \hbar_\infty$ is bounded and strictly decreasing with $\hbar_\infty \le \hbar(t) \le \hbar_0$. And $\hbar_0 > \hbar_\infty > 0$, $l > 0$, $0 < \underline{\delta} < 1$, and $0 < \overline{\delta} < 1$ are design parameters [26].

If e remains within the prescribed bound of (12), the maximum overshoot of e is restrained less than max $\{\overline{\delta}\hbar_0, \underline{\delta}\hbar_0\}$, and the steady value is no more than max $\{\overline{\delta}\hbar_\infty, \underline{\delta}\hbar_\infty\}$. Thus, the transient performance and steady performance of e are guaranteed by choosing appropriate parameters for (12).

Considering that it is unable to devise controller directly based on (12), an error transfer function $\mu(\varepsilon(t)) = \overline{\delta}e^{\varepsilon(t)} - \underline{\delta}e^{-\varepsilon(t)}/e^{\varepsilon(t)} + e^{-\varepsilon(t)}$ is applied to transfer (12) into the following formulation [28].

$$e(t) = \mu(\varepsilon(t))\hbar(t), \tag{13}$$

where $\varepsilon(t)$ is transfer error.

Appropriately, (13) is equivalent illustrated by (12). Furthermore, $\mu(\varepsilon(t))$ is bounded and strictly increasing.

From (13), we have

$$\varepsilon(t) = \mu^{-1}(\varepsilon) = \frac{1}{2}\ln\left(\frac{e/\hbar + \underline{\delta}}{\overline{\delta} - e/\hbar}\right). \tag{14}$$

Furthermore, $\dot{\varepsilon}(t)$ is acquired as

$$\dot{\varepsilon}(t) = r\left[\dot{e} - e\frac{\dot{\hbar}(t)}{\hbar(t)}\right]. \tag{15}$$

With

$$\begin{aligned} \dot{\hbar}(t) &= -l(\hbar_0 - \hbar_\infty)e^{-lt} \in [-l(\hbar_0 - \hbar_\infty), 0], \\ r &= \frac{1}{2\hbar(t)}\left[\frac{1}{e/\hbar(t) + \underline{\delta}} - \frac{1}{e/\hbar(t) - \overline{\delta}}\right] \\ &= \frac{1}{2\hbar(t)}\left[\frac{1}{\mu(\varepsilon(t)) + \underline{\delta}} - \frac{1}{\mu(\varepsilon(t)) - \overline{\delta}}\right]. \end{aligned} \tag{16}$$

It is obvious that r is bounded.

3.4. Backstepping Prescribed Performance Controller Design for GSP

3.4.1. Model Transformation. The first step of controller design is to transfer the mathematical model in (1). The mathematical model will be transferred into pure-feedback formation.

Define $y_1 = x_1$, $y_2 = x_2$, and $y_3 = (C_m x_3/J_L) - (T_{\text{turb}}/J_L)$, then we have

$$\begin{cases} \dot{y}_1 = y_2, \\ \dot{y}_2 = y_3, \\ \dot{y}_3 = f_1(y_2, y_3) + f_2(v) + f_d, \end{cases} \tag{17}$$

where $f_1(y_2, y_3) = (-(C_e/L_a)y_2 - (R_a J_L/L_a C_m)y_3)C_m/J_L$, and $f_2(v) = (C_m k_{\text{PWM}}/J_L L_a)(cv(t) + d(v))$ is control item, while $f_d = (C_m/J_L)(-(C_e/L_a)\dot{\vartheta} - (\dot{T}_{\text{turb}}/C_m) - (R_a/C_m L_a)T_{\text{turb}})$ represents transferred disturbance.

Then, separating the linear part of control item from nonlinear part, the following equation is acquired.

$$\begin{cases} \dot{y}_1 = y_2, \\ \dot{y}_2 = y_3, \\ \dot{y}_3 = f_1(y_2, y_3) + Acv(t) + f_{2d}(v) + f_d, \end{cases} \tag{18}$$

where the constant $A = C_m k_{\text{PWM}}/J_L L_a$, c is unknown gain, and $f_{2d} = (C_m k_{\text{PWM}}/J_L L_a)d(v)$ is unknown function regarded as disturbance to be estimated.

Remark 4. Aiming at the problem of unknown complex disturbances, a RBFNN will be adopted. Because of unknown control directions, RBFNN cannot be applied directly. Through equivalent transformation, unknown gain c becomes a part of unknown functions to be estimated.

Thus, the model of GSP in (1) is transformed into pure-feedback system in (18).

3.4.2. Control Law Design

Assumption 2. We assume that the angle reference signal θ_d is limited, while its derivative and its second-order derivative are also limited. Furthermore, the disturbance of basement $\dot{\vartheta}$ is also limited.

Step 1. Define the angle tracking error e_1.

$$e_1 = y_1 - y_{1d}. \tag{19}$$

Define a performance function $\hbar_1(t) = (\hbar_{01} - \hbar_{1\infty})e^{-l_1 t} + \hbar_{1\infty}$ to restrain e_1.

$$-\underline{\delta}_1\hbar_1(t) < e_1(t) < \overline{\delta}_1\hbar_1(t), \tag{20}$$

where $\hbar_{01} > 0$, $\hbar_{1\infty} > 0$, $l_1 > 0$, $0 < \underline{\delta_1} < 1$, and $0 < \overline{\delta_1} < 1$ are design parameters and satisfying $\hbar_{01} > \hbar_{1\infty}$, $-\underline{\delta_1}\hbar_1(t) < e_1(0) < \overline{\delta_1}\hbar_1(t)$, and $\hbar_{1\infty} < \hbar_1(t) < \hbar_{10}$.

We convert (20) into the following formulation:

$$e_1 = \mu_1(\varepsilon_1(t))\hbar_1(t), \tag{21}$$

where $\mu_1(\varepsilon_1(t)) = (\overline{\delta_1}e^{\varepsilon_1(t)} - \underline{\delta_1}e^{-\varepsilon_1(t)}/e^{\varepsilon_1(t)} + e^{-\varepsilon_1(t)}) \in (-\underline{\delta_1}, \overline{\delta_1})$ is a transformed function and $\varepsilon_1(t)$ is transformed error. From (14), we get the formulation of $\varepsilon_1(t)$

$$\varepsilon_1(t) = \mu_1^{-1}(\varepsilon_1(t)) = \frac{1}{2}\ln\left(\frac{e_1/\hbar_1(t) + \underline{\delta_1}}{\overline{\delta_1} - e_1/\hbar_1(t)}\right). \tag{22}$$

Furthermore, $\dot{\varepsilon}_1(t)$ is derived as

$$\begin{aligned}\dot{\varepsilon}_1(t) &= r_1\left[\dot{e}_1 - e_1\frac{\dot{\hbar}_1(t)}{\hbar_1(t)}\right] = r_1\left[\dot{y}_1 - \dot{y}_{1d} - e_1\frac{\dot{\hbar}_1(t)}{\hbar_1(t)}\right]\\ &= r_1\left[y_2 - \dot{y}_{1d} - e_1\frac{\dot{\hbar}_1(t)}{\hbar_1(t)}\right],\end{aligned} \tag{23}$$

where $r_1 = 1/2\hbar_1(t)[(1/\underline{\delta_1}e_1/\hbar_1(t) + \underline{\delta_1}) - (1/\underline{\delta_1}e_1/\hbar_1(t) - \overline{\delta_1})] \geq (1/2\underline{\delta_1}\hbar_1(t)) + (1/2\overline{\delta_1}\hbar_1(t)) > 0$.

The virtual control law is designed as

$$z_{2d} = -k_1\varepsilon_1(t) + \dot{y}_{1d} + e_1\frac{\dot{\hbar}_1(t)}{\hbar_1(t)}, \tag{24}$$

where k_1 is a design parameter, $\dot{\hbar}_1(t) = -l_1(\hbar_{10} - \hbar_{1\infty})e^{-l_1 t}$.

Step 2. Define angular velocity tracking error e_2.

$$e_2 = y_2 - y_{2d}. \tag{25}$$

Construct a performance function $\hbar_2(t) = (\hbar_{02} - \hbar_{2\infty})e^{-l_2 t} + \hbar_{2\infty} > 0$ to restrain e_2.

$$-\underline{\delta_2}\hbar_2(t) < e_2(t) < \overline{\delta_2}\hbar_2(t). \tag{26}$$

where $\hbar_{02} > 0$, $\hbar_{2\infty} > 0$, $l_2 > 0$, $0 < \underline{\delta_2} < 1$, and $0 < \overline{\delta_2} < 1$ are design parameters and satisfying $\hbar_{02} > \hbar_{2\infty}$, $-\underline{\delta_2}\hbar_2(t) < e_2(0) < \overline{\delta_2}\hbar_2(t)$, and $\hbar_{2\infty} < \hbar_2(t) < \hbar_{20}$.

Equation (26) is further converted into the following formulation:

$$e_2 = \mu_2(\varepsilon_2(t))\hbar_2(t). \tag{27}$$

where $\mu_2(\varepsilon_2(t)) = (\overline{\delta_2}e^{\varepsilon_2(t)} - \underline{\delta_2}e^{-\varepsilon_2(t)}/e^{\varepsilon_2(t)} + e^{-\varepsilon_2(t)}) \in (-\underline{\delta_2}, \overline{\delta_2})$ is a transformed function and $\varepsilon_2(t)$ is transformed error. From (27), we can get

$$\varepsilon_2(t) = \mu_2^{-1}(\varepsilon_2(t)) = \frac{1}{2}\ln\left(\frac{e_2/\hbar_2(t) + \underline{\delta_2}}{\overline{\delta_2} - e_2/\hbar_2(t)}\right). \tag{28}$$

The time derivative of $\varepsilon_2(t)$ is

$$\begin{aligned}\dot{\varepsilon}_2(t) &= r_2\left[\dot{e}_2 - e_2\frac{\dot{\hbar}_2(t)}{\hbar_2(t)}\right] = r_2\left[\dot{y}_2 - \dot{y}_{2d} - e_2\frac{\dot{\hbar}_2(t)}{\hbar_2(t)}\right]\\ &= r_2\left[y_3 - \dot{y}_{2d} - e_2\frac{\dot{\hbar}_2(t)}{\hbar_2(t)}\right],\end{aligned} \tag{29}$$

where $r_2 = 1/2\hbar_2(t)[(1/\underline{\delta_2}e_2/\hbar_2(t) + \underline{\delta_2}) - (1/\underline{\delta_2}e_2/\hbar_2(t) - \overline{\delta_2})] \geq (1/2\underline{\delta_2}\hbar_2(t)) + (1/2\overline{\delta_2}\hbar_2(t)) > 0$.

The virtual control law is devised as

$$y_{3d} = -k_2\varepsilon_2(t) + \dot{y}_{2d} + e_2\frac{\dot{\hbar}_2(t)}{\hbar_2(t)}, \tag{30}$$

where k_2 is a design parameter, $\dot{\hbar}_2(t) = -l_2(\hbar_{20} - \hbar_{2\infty})e^{-l_2 t}$.

Step 3. Define current tracking error e_3.

$$e_3 = y_3 - y_{3d}. \tag{31}$$

Construct a performance function $\hbar_3(t) = (\hbar_{03} - \hbar_{3\infty})e^{-l_3 t} + \hbar_{3\infty} > 0$ to restrain e_3.

$$-\underline{\delta_3}\hbar_3(t) < e_3(t) < \overline{\delta_3}\hbar_3(t), \tag{32}$$

where $\hbar_{03} > 0$, $\hbar_{3\infty} > 0$, $l_3 > 0$, $0 < \underline{\delta_3} < 1$, and $0 < \overline{\delta_3} < 1$ are design parameters and satisfying $\hbar_{03} > \hbar_{3\infty}$, $-\underline{\delta_3}\hbar_3(t) < e_3(0) < \overline{\delta_3}\hbar_3(t)$, and $\hbar_{3\infty} < \hbar_3(t) < \hbar_{30}$.

Equation (28) is further converted into the following formulation:

$$e_3 = \mu_3(\varepsilon_3(t))\hbar_3(t), \tag{33}$$

where $\mu_3(\varepsilon_3(t)) = (\overline{\delta_3}e^{\varepsilon_3(t)} - \underline{\delta_3}e^{-\varepsilon_3(t)}/e^{\varepsilon_3(t)} + e^{-\varepsilon_3(t)}) \in (-\underline{\delta_3}, \overline{\delta_3})$ is a transformed function and $\varepsilon_3(t)$ is transformed error. From (33), we can get

$$\varepsilon_3(t) = \mu_3^{-1}(\varepsilon_3(t)) = \frac{1}{2}\ln\left(\frac{e_3/\hbar_3(t) + \underline{\delta_3}}{\overline{\delta_3} - e_3/\hbar_3(t)}\right). \tag{34}$$

The time derivative of $\varepsilon_3(t)$ is

$$\begin{aligned}\dot{\varepsilon}_3(t) &= r_3\left[\dot{e}_3 - e_3\frac{\dot{\hbar}_3(t)}{\hbar_3(t)}\right] = r_3\left[\dot{y}_3 - \dot{y}_{3d} - e_3\frac{\dot{\hbar}_3(t)}{\hbar_3(t)}\right]\\ &= r_3\left[f_1(y_2, y_3) + Acv(t) + f_{2d}(v) + f_d - \dot{y}_{3d} - e_3\frac{\dot{\hbar}_3(t)}{\hbar_3(t)}\right],\end{aligned} \tag{35}$$

where $r_3 = 1/2\hbar_3(t)[(1/(\underline{\delta_3}e_3/\hbar_3(t) + \underline{\delta_3})) - (1/(\underline{\delta_3}e_3/\hbar_3(t) - \overline{\delta_3}))] \geq (1/2\underline{\delta_3}\hbar_3(t)) + (1/2\overline{\delta_3}\hbar_3(t)) > 0$.

Define Lyapunov function

$$V = \frac{\varepsilon_1^2}{2} + \frac{\varepsilon_2^2}{2} + \frac{\varepsilon_3^2}{2} + \frac{1}{\gamma_1}\tilde{\mathbf{W}}^T\dot{\tilde{\mathbf{W}}}. \tag{36}$$

Employing (23), (29), and (35), $\dot{V}$ is acquired as follows:

$$\begin{aligned}\dot{V} &= \varepsilon_1\dot{\varepsilon}_1 + \varepsilon_2\dot{\varepsilon}_2 + \varepsilon_3\dot{\varepsilon}_3 + \frac{1}{\gamma_1}\tilde{\mathbf{W}}^T\dot{\tilde{\mathbf{W}}} = \varepsilon_1 r_1\left[y_2 - \dot{y}_{1d} - e_1\frac{\dot{\hbar}_1}{\hbar_1}\right] \\ &\quad + \varepsilon_2 r_2\left[y_3 - \dot{y}_{2d} - e_2\frac{\dot{\hbar}_2}{\hbar_2}\right] + \varepsilon_3 r_3\left[f_1(y_2, y_3) + Acv(t)\right. \\ &\quad \left. + f_{2d}(v) + f_d - \dot{y}_{3d} - \mu_3\dot{\hbar}_3(t)\right] + \frac{1}{\gamma_1}\tilde{\mathbf{W}}^T\dot{\tilde{\mathbf{W}}} \\ &= \varepsilon_1 r_1\left[y_2 - \dot{y}_{1d} - e_1\frac{\dot{\hbar}_1}{\hbar_1}\right] + \varepsilon_2 r_2\left[y_3 - \dot{y}_{2d} - e_2\frac{\dot{\hbar}_2}{\hbar_2}\right] \\ &\quad + \varepsilon_3 r_3 Acv(t) + \varepsilon_3 r_3\left[f_1(y_2, y_3) - \dot{y}_{3d} - \mu_3\dot{\hbar}_3(t)\right] \\ &\quad + \varepsilon_3 r_3[f_{2d}(v) + f_d] + \frac{1}{\gamma_1}\tilde{\mathbf{W}}^T\dot{\tilde{\mathbf{W}}}.\end{aligned} \tag{37}$$

Here, a RBFNN is applied to offset the disturbance f_d as well as the unknown input function $f_{2d}(v)$. Considering that the input of the system contains an unknown gain c, RBFNN cannot be applied directly. Through an equivalent transformation, the following equation is acquired.

Remark 5. The unknown compound disturbance is $D = (f_d + f_{2d}(v))/Ac$, where $f_d = C_m/J_L(-(C_e/L_a)\dot{\vartheta} - (\dot{T}_{\text{turb}}/C_m) - (R_a/C_mL_a)T_{\text{turb}})$, $f_{2d} = (C_m k_{\text{PWM}}/J_L L_a)d(v)$, T_{turb} is friction disturbance, and it is one part of unknown compound disturbance. Besides, the unknown function of unknown hysteresis $d(v)$ is estimated too. The compound disturbance will be estimated in whole.

$$\begin{aligned}\dot{V} &= \varepsilon_1 r_1\left[y_2 - \dot{y}_{1d} - e_1\frac{\dot{\hbar}_1}{\hbar_1}\right] + \varepsilon_2 r_2\left[y_3 - \dot{y}_{2d} - e_2\frac{\dot{\hbar}_2}{\hbar_2}\right] \\ &\quad + \varepsilon_3 r_3 Ac\left(v_1(t) - \widehat{\mathbf{W}}\mathbf{h}(\boldsymbol{x})\right) + \varepsilon_3 r_3\left[f_1(y_2, y_3) - \dot{y}_{3d} - \mu_3\dot{\hbar}_3(t)\right] \\ &\quad + \varepsilon_3 r_3[f_{2d}(v) + f_d] + \frac{1}{\gamma_1}\tilde{\mathbf{W}}^T\dot{\tilde{\mathbf{W}}} = \varepsilon_1 r_1\left[y_2 - \dot{y}_{1d} - e_1\frac{\dot{\hbar}_1}{\hbar_1}\right] \\ &\quad + \varepsilon_2 r_2\left[y_3 - \dot{y}_{2d} - e_2\frac{\dot{\hbar}_2}{\hbar_2}\right] + \varepsilon_3 r_3\left[f_1(y_2, y_3) - \dot{y}_{3d} - \mu_3\dot{\hbar}_3(t)\right] \\ &\quad + \varepsilon_3 r_3 Acv_1(t) + \varepsilon_3 r_3 Ac\left(-\widehat{\mathbf{W}}\mathbf{h}(\mathbf{x}) + \frac{(f_{2d}(v) + f_d)}{A}c\right) \\ &\quad + \frac{1}{\gamma_1}\tilde{\mathbf{W}}^T\dot{\tilde{\mathbf{W}}}.\end{aligned} \tag{38}$$

Substituting (19), (25), and (31) into (38) leads to

$$\begin{aligned}\dot{V} &= \varepsilon_1(t)r_1[e_2 - k_1\varepsilon_1] + \varepsilon_2(t)r_2[e_3 - k_2\varepsilon_2(t)] \\ &\quad + \varepsilon_3(t)r_3 Ac\left(v_1(t) - \widehat{\mathbf{W}}\mathbf{h}(\mathbf{x})\right) \\ &\quad + \varepsilon_3(t)r_3\left[f_1(y_2, y_3) - \dot{y}_{3d} - \mu_3\dot{\hbar}_3(t)\right] \\ &\quad + \varepsilon_3(t)r_3[f_{2d}(v) + f_d] + \frac{1}{\gamma_1}\tilde{\mathbf{W}}^T\dot{\tilde{\mathbf{W}}} \\ &= r_1\left[\mu_2(\varepsilon_2)\hbar_2(t)\varepsilon_1(t) - k_1\varepsilon_1^2(t)\right] \\ &\quad + r_2\left[\mu_3(\varepsilon_3)\hbar_3(t)\varepsilon_2(t) - k_2\varepsilon_2^2(t)\right] \\ &\quad + \varepsilon_3 r_3 Ac\left(v_1(t) - \widehat{\mathbf{W}}\mathbf{h}(\mathbf{x})\right) \\ &\quad + \varepsilon_3 r_3\left[f_1(y_2, y_3) - \dot{y}_{3d} - \mu_3\dot{\hbar}_3(t)\right] \\ &\quad + \varepsilon_3 r_3[f_{2d}(v) + f_d] + \frac{1}{\gamma_1}\tilde{\mathbf{W}}^T\dot{\tilde{\mathbf{W}}}.\end{aligned} \tag{39}$$

Define a total disturbance $D = (f_d + f_{2d}(v))/Ac$, we mean that $D = \widehat{\mathbf{W}}\mathbf{h}(\mathbf{x}) + \varepsilon$, where $\mathbf{x} = [x_1, x_2, x_3]$. That is to say, when ε is small enough, $\widehat{\mathbf{W}}\mathbf{h}(\mathbf{x})$ will converge to D in high precision [26]. Thus, $v(t) = v_1(t) - \widehat{\mathbf{W}}\mathbf{h}(\mathbf{x})$.

To analyze disturbance item individually, define a new function as follows.

$$\begin{aligned}\dot{V}_d &= \varepsilon_3 r_3 Ac\left(-\widehat{\mathbf{W}}\mathbf{h}(\mathbf{x}) + \frac{(f_{2d}(v) + f_d)}{Ac}\right) + \frac{1}{\gamma_1}\tilde{\mathbf{W}}^T\dot{\tilde{\mathbf{W}}} \\ &\leq \varepsilon_3 r_3 Ac\left(\tilde{\mathbf{W}}\mathbf{h}(\mathbf{x}) + \varepsilon_{\max}\right) + \frac{1}{\gamma_1}\tilde{\mathbf{W}}^T\dot{\tilde{\mathbf{W}}}.\end{aligned} \tag{40}$$

Define a positive constant $\bar{c}$ satisfying $|c| \leq \bar{c}$. Applying Young's inequality [24], we can acquire that

$$\begin{aligned}\dot{V}_d &\leq \frac{\left(\tilde{\mathbf{W}}\mathbf{h}(\mathbf{x}) + \varepsilon_{\max}\right)^2}{2} + \frac{(\varepsilon_3 r_3 A\bar{c})^2}{2} + \frac{1}{\gamma_1}\tilde{\mathbf{W}}^T\dot{\tilde{\mathbf{W}}} = \frac{\varepsilon_{\max}^2}{2} \\ &\quad + \frac{(\varepsilon_3 r_3 A\bar{c})^2}{2} + \tilde{\mathbf{W}}^T\left(\frac{\tilde{\mathbf{W}}\mathbf{h}(\mathbf{x})^T\mathbf{h}(\mathbf{x})}{2} + \varepsilon_{\max}\mathbf{h}(\mathbf{x}) + \frac{\dot{\tilde{\mathbf{W}}}}{\gamma_1}\right).\end{aligned} \tag{41}$$

Since $\mathbf{W}^*$ is a constant, it should be noted that $\dot{\tilde{\mathbf{W}}} = \dot{\hat{\mathbf{W}}}$. According to (41), adaption law $\dot{\hat{\mathbf{W}}}$ is designed as follows:

$$\dot{\tilde{\mathbf{W}}} = -\gamma_1\left(\frac{\tilde{\mathbf{W}}\mathbf{h}(\mathbf{x})^T\mathbf{h}(\mathbf{x})}{2} + \varepsilon_{\max}\mathbf{h}(\mathbf{x})\right). \tag{42}$$

Then, (41) becomes

$$\dot{V}_d \leq \frac{\varepsilon_{\max}^2}{2} + \frac{(\varepsilon_3 r_3 A\bar{c})^2}{2}. \tag{43}$$

Combining with (39), the following inequality is acquired.

$$\begin{aligned}\dot{V} \le\ & r_1\left[\mu_2(\varepsilon_2)\hbar_2(t)\varepsilon_1(t) - k_1{\varepsilon_1}^2(t)\right] \\ & + r_2\left[\mu_3(\varepsilon_3)\hbar_3(t)\varepsilon_2(t) - k_2{\varepsilon_2}^2(t)\right] \\ & + \varepsilon_3 r_3\left[f_1(y_2, y_3) - \dot{y}_{3d} - \mu_3\dot{\hbar}_3(t)\right] \\ & + \varepsilon_3 r_3 Acv_1(t) + \frac{{\varepsilon_{\max}}^2}{2} + \frac{(\varepsilon_3 r_3 A\bar{c})^2}{2}.\end{aligned} \tag{44}$$

It is not hard to conclude that there exists a positive constant $\sum_0$ such that $|f_1(y_2, y_3) - \dot{y}_{3d} - \mu_3\dot{\hbar}_3(t)| \le \sum_0$. Furthermore, we know that $\hbar_{2\infty} < \hbar_2(t) < \hbar_{20}, \hbar_{3\infty} < \hbar_3(t) < \hbar_{30}$, $r_1 \ge (1/2\hbar_1(t))((1/\delta_1) + (1/\delta_1)) > 0$, $r_2 \ge (1/2\hbar_2(t))((1/\delta_2) + (1/\overline{\delta_2})) > 0$, $\mu_2(\varepsilon_2(t)) = (\overline{\delta}_2 e^{\varepsilon_2(t)} - \underline{\delta_2} e^{-\varepsilon_2(t)}/e^{\varepsilon_2(t)} + e^{-\varepsilon_2(t)}) \in (-\underline{\delta_2}, \overline{\delta_2})$, $\mu_3(\varepsilon_3(t)) = (\overline{\delta}_3 e^{\varepsilon_3(t)} - \underline{\delta_3} e^{-\varepsilon_3(t)}/e^{\varepsilon_3(t)} + e^{-\varepsilon_3(t)}) \in (-\underline{\delta_3}, \overline{\delta_3})$.

Then (44) becomes

$$\begin{aligned}\dot{V} \le\ & r_1|\varepsilon_1(t)|\left[\overline{\delta}_2\hbar_2(t) - k_1|\varepsilon_1(t)|\right] \\ & + r_2|\varepsilon_2(t)|\left[\overline{\delta}_3\hbar_3(t) - k_2|\varepsilon_2(t)|\right] \\ & + |\varepsilon_3| r_3 \sum_0 + \varepsilon_3 r_3 Acv_1(t) + \frac{{\varepsilon_{\max}}^2}{2} + \frac{(\varepsilon_3 r_3 A\bar{c})^2}{2}.\end{aligned} \tag{45}$$

Finally, the actual control law is chosen as

$$\begin{cases} v_1(t) = N_3(\xi_3)\left[\kappa_{31}\varepsilon_3(t) + \dfrac{\kappa_{32} r_3 \varepsilon_3(t)}{2}\right] \text{-}\widehat{\mathbf{W}}\mathbf{h}(\mathbf{x}), \\ \dot{\xi}_3 = \kappa_{31} r_3 {\varepsilon_3}^2(t) + \dfrac{\kappa_{32} {r_3}^2 {\varepsilon_3}^2(t)}{2}, \end{cases} \tag{46}$$

where $N_3(\xi_3) = e^{{\xi_3}^2} \cos(\pi\xi_3/2)$ is a Nussbaum function [30]; κ_{31} and κ_{32} are design parameters.

Invoking (41), (44) becomes

$$\begin{aligned}\dot{V} \le\ & r_1|\varepsilon_1(t)|\left[\overline{\delta}_2\hbar_2(t) - k_1|\varepsilon_1(t)|\right] \\ & + r_2|\varepsilon_2(t)|\left[\overline{\delta}_3\hbar_3(t) - k_2|\varepsilon_2(t)|\right] \\ & + |\varepsilon_3| r_3 \sum_0 + \varepsilon_3 r_3 AcN_3(\xi_3)\left[\kappa_{31}\varepsilon_3(t) + \frac{\kappa_{32} r_3 \varepsilon_3(t)}{2}\right] \\ & + \frac{{\varepsilon_{\max}}^2}{2} + \frac{(\varepsilon_3 r_3 A\bar{c})^2}{2}.\end{aligned} \tag{47}$$

Based on Young's inequality, it is easy to get $|\varepsilon_3(t)| r_3 \sum_0 \le (\kappa_{32} {r_3}^2 {\varepsilon_3}^2(t)/2) + ({\sum_0}^2/2\kappa_{32})$.

Then (47) becomes

$$\begin{aligned}\dot{V} \le\ & r_1|\varepsilon_1(t)|\left[\overline{\delta}_2\hbar_2(t) - k_1|\varepsilon_1(t)|\right] \\ & + r_2|\varepsilon_2(t)|\left[\overline{\delta}_3\hbar_3(t) - k_2|\varepsilon_2(t)|\right] \\ & + \frac{\kappa_{32} {r_3}^2 {\varepsilon_3}^2(t)}{2} + \frac{{\sum_0}^2}{2\kappa_{32}} \\ & + \varepsilon_3 r_3 AcN_3(\xi_3)\left[\kappa_{31}\varepsilon_3(t) + \frac{\kappa_{32} r_3 \varepsilon_3(t)}{2}\right] \\ & + \frac{{\varepsilon_{\max}}^2}{2} + \frac{(\varepsilon_3 r_3 A\bar{c})^2}{2} = r_1|\varepsilon_1(t)|\left[\overline{\delta}_2\hbar_2(t) - k_1|\varepsilon_1(t)|\right] \\ & + r_2|\varepsilon_2(t)|\left[\overline{\delta}_3\hbar_3(t) - k_2|\varepsilon_2(t)|\right] + + \frac{\kappa_{32} {r_3}^2 {\varepsilon_3}^2(t)}{2} \\ & + \frac{{\sum_0}^2}{2\kappa_{32}} + AcN_3(\xi_3)\dot{\xi}_3 + \frac{{\varepsilon_{\max}}^2}{2} + \frac{(\varepsilon_3 r_3 A\bar{c})^2}{2} \\ =\ & r_1|\varepsilon_1(t)|\left[\overline{\delta}_2\hbar_2(t) - k_1|\varepsilon_1(t)|\right] \\ & + r_2|\varepsilon_2(t)|\left[\overline{\delta}_3\hbar_3(t) - k_2|\varepsilon_2(t)|\right] + -\kappa_{31} {r_3}^2 {\varepsilon_3}^2(t) \\ & + \kappa_{31} {r_3}^2 {\varepsilon_3}^2(t) + \frac{\kappa_{32} {r_3}^2 {\varepsilon_3}^2(t)}{2} + \frac{{\sum_0}^2}{2\kappa_{32}} + AcN_3(\xi_3)\dot{\xi}_3 \\ & + \frac{{\varepsilon_{\max}}^2}{2} + \frac{(\varepsilon_3 r_3 A\bar{c})^2}{2} = r_1|\varepsilon_1(t)|\left[\overline{\delta}_2\hbar_2(t) - k_1|\varepsilon_1(t)|\right] \\ & + r_2|\varepsilon_2(t)|\left[\overline{\delta}_3\hbar_3(t) - k_2|\varepsilon_2(t)|\right] + AcN_3(\xi_3)\dot{\xi}_3 + \dot{\xi}_3 \\ & - \kappa_{31} {r_3}^2 {\varepsilon_3}^2(t) + \frac{{\sum_0}^2}{2\kappa_{32}} + \frac{{\varepsilon_{\max}}^2}{2} + \frac{(\varepsilon_3 r_3 A\bar{c})^2}{2}.\end{aligned} \tag{48}$$

It is obvious to observe from (48) that $\varepsilon_1(t)$ and $\varepsilon_2(t)$ are bounded if $|\varepsilon_1(t)| \le \overline{\delta}_2\hbar_{20}/k_1$ and $|\varepsilon_2(t)| \le \overline{\delta}_3\hbar_{30}/k_2$. Else if $|\varepsilon_1(t)| > \overline{\delta}_2\hbar_{20}/k_1$ and $|\varepsilon_2(t)| > \overline{\delta}_3\hbar_{30}/k_2$, we obtain $r_1|\varepsilon_1(t)|[\overline{\delta}_2\hbar_{20} - k_1|\varepsilon_1(t)|] < 0$ and $r_2|\varepsilon_2(t)|[\overline{\delta}_3\hbar_{30} - k_2|\varepsilon_2(t)|] < 0$. Moreover, there exist adequately small constants $0 < k_3 < r_1 k_1$ and $0 < k_4 < r_2 k_2$ such that $r_1|\varepsilon_1(t)|[\overline{\delta}_2\hbar_{20} - k_1|\varepsilon_1(t)|] + k_3 {\varepsilon_1}^2(t) < 0$ and $r_2|\varepsilon_2(t)|[\overline{\delta}_3\hbar_{30} - k_2|\varepsilon_2(t)|] + k_4{\varepsilon_2}^2(t) < 0$.

Thus, (48) becomes

$$\begin{aligned}\dot{V} \le\ & r_1|\varepsilon_1(t)|\left[\overline{\delta}_2\hbar_2(t) - k_1|\varepsilon_1(t)|\right] + k_3{\varepsilon_1}^2(t) - k_3{\varepsilon_1}^2(t) \\ & + r_2|\varepsilon_2(t)|\left[\overline{\delta}_3\hbar_3(t) - k_2|\varepsilon_2(t)|\right] + k_4{\varepsilon_2}^2(t) - k_4{\varepsilon_2}^2(t) \\ & + AcN_3(\xi_3)\dot{\xi}_3 + \dot{\xi}_3 - \kappa_{31} {r_3}^2 {\varepsilon_3}^2(t) + \frac{{\sum_0}^2}{2\kappa_{32}} + \frac{{\varepsilon_{\max}}^2}{2} \\ & + \frac{(\varepsilon_3 r_3 A\bar{c})^2}{2} \le -k_3{\varepsilon_1}^2(t) - k_4{\varepsilon_2}^2(t) \\ & - \left(\kappa_{31} - \frac{(A\bar{c})^2}{2}\right) {r_3}^2 {\varepsilon_3}^2(t) + AcN_3(\xi_3)\dot{\xi}_3 + \dot{\xi}_3 + \frac{{\sum_0}^2}{2\kappa_{32}} \\ & + \frac{{\varepsilon_{\max}}^2}{2} \le -\iota_h V + AcN_3(\xi_3)\dot{\xi}_3 + \dot{\xi}_3 + \frac{{\sum_0}^2}{2\kappa_{32}} + \frac{{\varepsilon_{\max}}^2}{2}.\end{aligned} \tag{49}$$

With $\iota_1 = \min\{2k_3, 2k_4, \kappa_{31}r_3 - ((r_3 A\bar{c})/2)^2\}$, $\kappa_{31} > (r_3(A\bar{c})/2)^2$.

Multiplying $e^{\iota_1 t}$ on both sides of (49) leads to

$$\frac{d}{dx}\left(Ve^{\iota_1 t}\right) \le AcN_3(\xi_3)\dot{\xi}_3 e^{\iota_1 t} + \dot{\xi}_3 e^{\iota_1 t} + \frac{\sum_0^2}{2\kappa_{32}} + \frac{\varepsilon_{\max}^2}{2}. \quad (50)$$

Integrating (45) over $[0, t]$, we obtain

$$0 \le V \le V(0) + e^{-\iota_1 t}\int_0^t AcN_3(\xi_3)\dot{\xi}_3 e^{\iota_1 \tau}d\tau + e^{-\iota_1 t}\int_0^t \dot{\xi}_3 e^{\iota_1 \tau}d\tau + \int_0^t \left(\frac{\sum_0^2}{2\kappa_{32}} + \frac{\varepsilon_{\max}^2}{2}\right)e^{-\iota_1(t-\tau)}d\tau. \quad (51)$$

Noticing $\int_0^t((\sum_0^2/2\kappa_{32}) + (\delta_{\max}/2)^2)e^{-\iota_1(t-\tau)}d\tau = ((\sum_0^2/2\kappa_{32}) + (\varepsilon_{\max}/2)^2)(1/\iota_1)(1 - e^{-\iota_1 t}) \in [0, (\sum_0^2/2\kappa_{32}) + (\varepsilon_{\max}/2)^2)$, we know that $\int_0^t((\sum_0^2/2\kappa_{32}) + (\varepsilon_{\max}/2)^2)e^{-\iota_1(t-\tau)}d\tau$ is bounded. Furthermore, (46) becomes

$$0 \le V \le V(0) + \frac{\sum_0^2}{2\kappa_{32}} + \frac{\varepsilon_{\max}^2}{2} + e^{-\iota_1 t}\int_0^t AcN_3(\xi_3)\dot{\xi}_3 e^{\iota_1 \tau}d\tau + e^{-\iota_1 t}\int_0^t \dot{\xi}_3 e^{\iota_1 \tau}d\tau. \quad (52)$$

Invoking lemmas 1 and 2 presented in [30, 31], we know that V, $e^{-\iota_1 t}\int_0^t AcN_3(\xi_3)\dot{\xi}_3 e^{\iota_1 \tau}d\tau$, and $e^{-\iota_1 t}\int_0^t \dot{\xi}_3 e^{\iota_1 \tau}d\tau$ are all bounded. Thus, all the signals involved are bounded. From the boundedness of ε_1, ε_2, and ε_3, we know that there exist positive constants $\bar{\varepsilon}_1, \bar{\varepsilon}_2, \bar{\varepsilon}_3$ such that $|\varepsilon_1| \le \bar{\varepsilon}_1$, $|\varepsilon_2| \le \bar{\varepsilon}_2$, and $|\varepsilon_3| \le \bar{\varepsilon}_3$. Furthermore, $-\underline{\delta}_i\hbar_i(t) < (-\bar{\delta}_i e^{\varepsilon_i(t)} + \underline{\delta}_i e^{-\varepsilon_i(t)}/e^{\varepsilon_i(t)} + e^{-\varepsilon_i(t)})\hbar_i(t) \le e_i(t) \le (\bar{\delta}_i e^{\varepsilon_i(t)} - \underline{\delta}_i e^{-\varepsilon_i(t)}/e^{\varepsilon_i(t)} + e^{-\varepsilon_i(t)})\hbar_i(t) < \bar{\delta}_i\hbar_i(t)$, $i = 1, 2, 3$. It is obvious that the prescribed performance for e_1, e_2, and e_3 is guaranteed.

The design procedure of GSP is completed.

Remark 6. It should be noted that the controller design is not relying on model of GSP, which guarantees the robustness against model uncertain and unknown disturbance.

Remark 7. Though similar control framework is designed as reference [31], compared with [31], the robustness against compound disturbances and unknown control directions is enhanced in large scale. Especially, the stability of system under compound disturbances is proven. However, in [31], the stability analysis as well as controller design did not consider any disturbances, which was not rigorous.

4. Simulation and Analysis

To verify the effectiveness of the proposed control scheme, a seeker servo system is chosen as simulation case.

The parameters of the control plant are shown in Table 1.

Table 1: Model Parameters.

Parameter	Value	Parameter	Value
J_L	1.2×10^{-3}kg · m^2	C_e	0.75
C_m	0.625N · m/A	v_s	0.2
L_a	0.0062H	F_C	0.03
R_a	5.1Ω	F_S	0.05
k_{PWM}	3.75	B_v	0.017

The control parameters of controller are chosen as follows: $k_1 = 20$, $k_2 = 15$, $\kappa_{31} = -6$, $\kappa_{32} = 3$, $\overline{\delta_1} = 1$, $\underline{\delta_1} = 1$, $\hbar_{01} = 5$, $\hbar_{1\infty} = 0.1$, $l_1 = 0.6$, $\overline{\delta_2} = 1$, $\underline{\delta_2} = 1$, $\hbar_{02} = 15$, $\hbar_{2\infty} = 0.15$, $l_2 = 0.5$, $\overline{\delta_3} = 1$, $\underline{\delta_3} = 1$, $\hbar_{03} = 30$, $\hbar_{3\infty} = 5$, and $l_3 = 0.3$. Moreover, all the model coefficients in (1) are assumed to be uncertain by defining $C = C_0(1 + 0.3\cos(2t))$, where C is the uncertain coefficient and C_0 is the nominal value of C. While the parameters of RBFNN are chosen as $\gamma_1 = 100$, $\varepsilon_{\max} = 0.001$, the number of node is 100, and the center of RBFNN is evenly spaced in $\boldsymbol{c} \in [-5, 4.9]$, the width is chosen as $b = 10$.

We choose $\sin(t)$ as angular reference signal, while the initial disalignment angle is 0.5rad. Because the GSP possesses great isolation towards high-frequency signals [32], the basement disturbance is $\dot{\vartheta} = 0.5\cos(2t)$(rad/$s$). The tracking performance of the presented control approach is depicted in Figures 3–6.

Figures 4–6 show that all tracking errors are forced within the prescribed bounds in the presence of compound disturbances. Thus, the control object is achieved. Furthermore, we can observer from Figures 4 and 5 that the system output of the proposed method converges faster and the precision is higher. Results show that the steady error of angle and angular velocity are no more than 0.02rad and 0.12rad/s, respectively. It indicates that better transient and steady performance can be achieved through designed controller. Besides, the controller output is shown in Figure 7; because of nonlinear friction disturbance, the controller output is nonsmooth at velocity zero point. Especially, the designed controller is independent of precise model, and the method is able to achieve off-line estimation of unknown certain disturbance and the method enables great robustness against uncertain disturbance.

5. Conclusion

In this paper, a prescribed performance controller based on RBFNN is exploited for GSP with the backstepping framework. The problem of unknown hysteresis, unknown friction, and unknown compound disturbance is solved through a model transformation and RBFNN estimation of compound disturbances. Furthermore, Nussbaum function is adopted in this paper, which overcomes the problem of GSP with "unknown control directions". By constructing performance functions, angle and angular velocity tracking errors are restrained within the prescribed boundaries. The stability of the proposed method is proved via Lyapunov stability synthesis. Finally, the tracking performance and

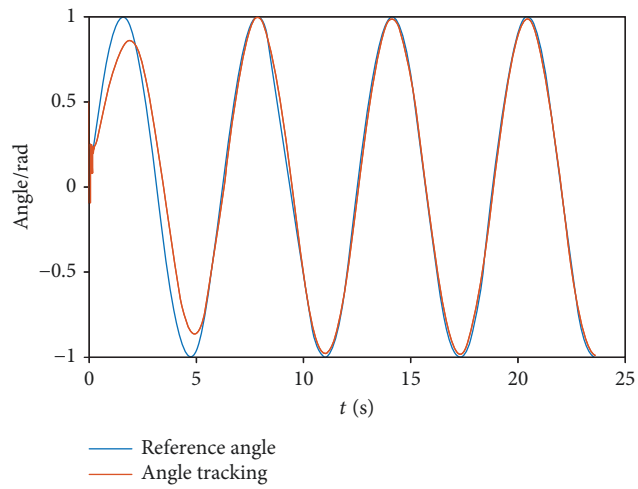

Figure 3: Angle tracking performance.

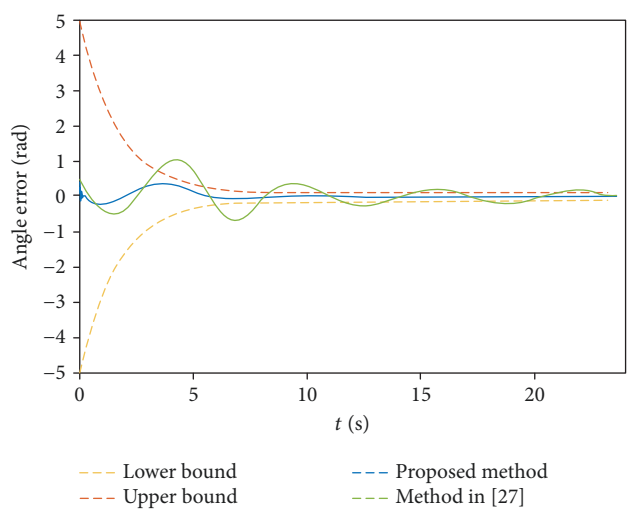

Figure 4: Angle tracking error.

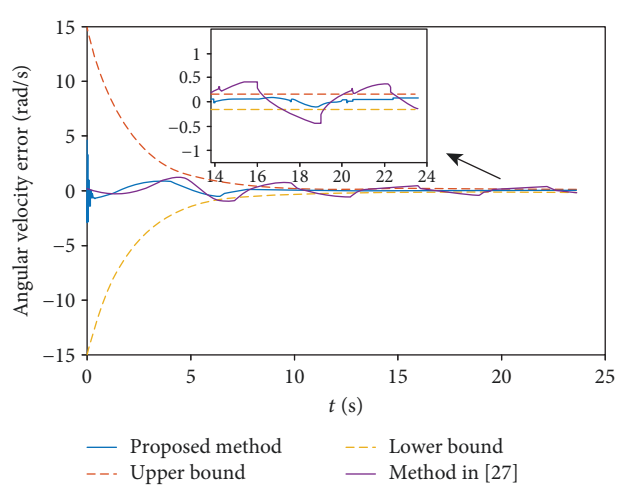

Figure 5: Angular velocity tracking error.

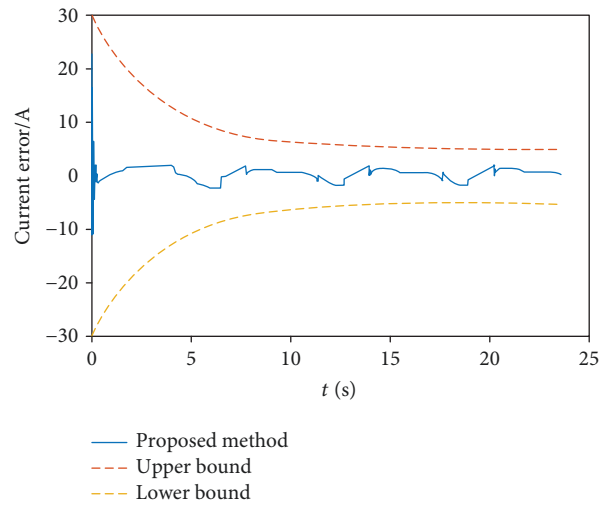

Figure 6: Current tracking error.

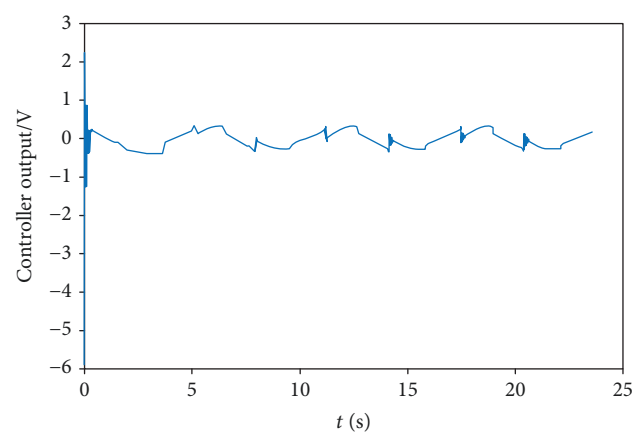

Figure 7: Controller output.

superiority of the designed method are proved through simulations. Especially, the research of GSP can be improved by considering interactions between gimbals, which will be more meaningful in practical systems.

Data Availability

The data used to support the findings of this study are included within the article.

Conflicts of Interest

The authors declare that they have no conflicts of interest.

Acknowledgments

This work was supported by the Natural Science Foundation of China (grant No: 61573374, No: 61503408, No: 61703421, and No: 61773398).

References

[1] M. J. Stepaniak, M. U. de Haag, and F. Van Graas, "Field programmable gate array-based attitude stabilization," *Journal of Aerospace Computing, Information, and Communication*, vol. 6, no. 7, pp. 451–463, 2009.

[2] X. Zhou, B. Zhao, W. Liu, H. Yue, R. Yu, and Y. Zhao, "A compound scheme on parameters identification and adaptive compensation of nonlinear friction disturbance for the aerial inertially stabilized platform," *ISA Transactions*, vol. 67, pp. 293–305, 2017.

[3] D. Haarhoff, M. Kolditz, D. Abel, and S. Brell-Cokcan, "Actuator design for stabilizing single tendon platforms," in *New Advances in Mechanisms, Mechanical Transmissions and Robotics*, B. Corves, E. C. Lovasz, M. Hüsing, I. Maniu, and C. Gruescu, Eds., vol. 46, pp. 371–378, Springer, 2017.

[4] P. J. Kennedy and R. L. Kennedy, "Direct versus indirect line of sight stabilization," *IEEE Transactions on Control System Technology*, vol. 11, no. 8, pp. 1293–1299, 2003.

[5] H. Sun and S. M. Zhang, "Computation model and error budget for image motion of aerial imaging system," *Optics and Precision Engineering*, vol. 20, no. 11, pp. 2492–2499, 2012.

[6] Y. Zhang, T. Yang, C. Li et al., "Fuzzy-PID control for the position loop of aerial inertially stabilized platform," *Aerospace Science and Technology*, vol. 36, pp. 21–26, 2014.

[7] Y. Zou and X. Lei, "A compound control method based on the adaptive neural network and sliding mode control for inertial stable platform," *Neurocomputing*, vol. 155, pp. 286–294, 2015.

[8] X. Zhou, Y. Jia, Q. Zhao, and T. Cai, "Dual-rate-loop control based on disturbance observer of angular acceleration for a three-axis aerial inertially stabilized platform," *ISA Transactions*, vol. 63, pp. 288–298, 2016.

[9] Z. Zhang, Z. Li, Q. Zhou, L. Zhang, and D. Fan, "Application in prestiction friction compensation for angular velocity loop of inertially stabilized platforms," *Chinese Journal of Aeronautics*, vol. 27, no. 3, pp. 655–662, 2014.

[10] N. H. Giap, J. H. Shin, and W. H. Kim, "Robust adaptive neural network control for XY table," *Intelligent Control and Automation*, vol. 4, no. 3, pp. 293–300, 2013.

[11] X. Lei, Y. Zou, and F. Dong, "A composite control method based on the adaptive RBFNN feedback control and the ESO for two-axis inertially stabilized platforms," *ISA Transactions*, vol. 59, pp. 424–433, 2015.

[12] F. Dong, X. Lei, and W. Chou, "A dynamic model and control method for a two-axis inertially stabilized platform," *IEEE Transactions on Industrial Electronics*, vol. 64, no. 1, pp. 432–439, 2017.

[13] Z. Li, J. Shan, and U. Gabbert, "Inverse compensation of hysteresis using Krasnoselskii-Pokrovskii model," *IEEE/ASME Transactions on Mechatronics*, vol. 23, no. 2, pp. 966–971, 2018.

[14] M. al Janaideh and O. Aljanaideh, "Further results on open-loop compensation of rate-dependent hysteresis in a magnetostrictive actuator with the Prandtl-Ishlinskii model," *Mechanical Systems and Signal Processing*, vol. 104, pp. 835–850, 2018.

[15] H. Wang, B. Chen, K. Liu, X. Liu, and C. Lin, "Adaptive neural tracking control for a class of nonstrict-feedback stochastic nonlinear systems with unknown backlash-like hysteresis," *IEEE Transactions on Neural Networks and Learning Systems*, vol. 25, no. 5, pp. 947–958, 2014.

[16] Q. Ma, G. Cui, and T. Jiao, "Neural-network-based adaptive tracking control for a class of pure-feedback stochastic nonlinear systems with backlash-like hysteresis," *Neurocomputing*, vol. 144, pp. 501–508, 2014.

[17] Y. Li, S. Tong, and T. Li, "Adaptive fuzzy output feedback control of uncertain nonlinear systems with unknown backlash-like hysteresis," *Information Sciences*, vol. 198, pp. 130–146, 2012.

[18] Z. Yu, S. Li, Z. Yu, and F. Li, "Adaptive neural output feedback control for nonstrict-feedback stochastic nonlinear systems with unknown backlash-like hysteresis and unknown control directions," *IEEE Transactions on Neural Networks and Learning Systems*, vol. 29, no. 4, pp. 1147–1160, 2018.

[19] Y. Wang, H. Lei, J. Ye, and X. Bu, "Backstepping sliding mode control for radar seeker servo system considering guidance and control system," *Sensors*, vol. 18, no. 9, 2018.

[20] E. K. Gdoura, M. Feki, and N. Derbel, "Sliding mode control of a hydraulic servo system position using adaptive sliding surface and adaptive gain," *International Journal of Modelling, Identification and Control*, vol. 23, no. 3, p. 248, 2015.

[21] H. Hong, X. Zhou, Z. Zhang, and D. Fan, "Modeling and calibration of pointing errors using a semi-parametric regression method with applications in inertially stabilized platforms," *Proceedings of the Institution of Mechanical Engineers, Part B: Journal of Engineering Manufacture*, vol. 227, no. 10, pp. 1492–1503, 2013.

[22] C. Y. Su, Y. Stepanenko, J. Svoboda, and T. P. Leung, "Robust adaptive control of a class of nonlinear systems with unknown backlash-like hysteresis," *IEEE Transactions on Automatic Control*, vol. 45, no. 12, pp. 2427–2432, 2000.

[23] X. Du, T. Y. Liu, and Q. L. Xia, "Research of disturbance rejection effect performance of phased array seeker with platform for air-to-air missile," *System Engineering and Electronics*, vol. 39, no. 4, pp. 846–853, 2017.

[24] S. Li, M. Zhong, and Y. Zhao, "Estimation and compensation of unknown disturbance in three-axis gyro-stabilized camera mount," *Transactions of the Institute of Measurement and Control*, vol. 37, no. 6, pp. 732–745, 2015.

[25] X. Bu, X. Wu, J. Huang, and D. Wei, "A guaranteed transient performance-based adaptive neural control scheme with low-complexity computation for flexible air-breathing hypersonic vehicles," *Nonlinear Dynamics*, vol. 84, no. 4, pp. 2175–2194, 2016.

[26] X. Bu, X. Wu, M. Tian, J. Huang, R. Zhang, and Z. Ma, "High-order tracking differentiator based adaptive neural control of a flexible air-breathing hypersonic vehicle subject to actuators constraints," *ISA Transactions*, vol. 58, pp. 237–247, 2015.

[27] X. Bu, D. Wei, X. Wu, and J. Huang, "Guaranteeing preselected tracking quality for air-breathing hypersonic non-affine models with an unknown control direction via concise neural control," *Journal of the Franklin Institute*, vol. 353, no. 13, pp. 3207–3232, 2017.

[28] B. Xu, "Robust adaptive neural control of flexible hypersonic flight vehicle with dead-zone input nonlinearity," *Nonlinear Dynamics*, vol. 80, no. 3, pp. 1509–1520, 2015.

[29] X. Bu, "Air-breathing hypersonic vehicles funnel control using neural approximation of non-affine dynamics," *IEEE/ASME Transactions on Mechatronics*, vol. 23, no. 5, pp. 2099–2108, 2018.

[30] S. S. Ge, F. Hong, and T. H. Lee, "Adaptive neural control of nonlinear time-delay systems with unknown virtual control

coefficients," *IEEE Transactions on Systems, Man, and Cybernetics Part B: Cybernetics*, vol. 34, no. 1, pp. 499–516, 2004.

[31] X. Bu, "Guaranteeing prescribed output tracking performance for air-breathing hypersonic vehicles via non-affine backstepping control design," *Nonlinear Dynamics*, vol. 91, no. 1, pp. 525–538, 2018.

[32] B. Chen, X. Liu, K. Liu, and C. Lin, "Direct adaptive fuzzy control of nonlinear strict-feedback systems," *Automatica*, vol. 45, no. 6, pp. 1530–1535, 2009.